ELSEVIER

PII: S0032-3861(97)00003-7

Polymer Vol. 38 No. 19, pp. 4785–4794, 1997

0032-3861/97/$17.00 + 0.00

Non-destructive and localized assessment of acidic microenvironments inside biodegradable polyanhydrides by spectral spatial electron paramagnetic resonance imaging

Karsten Mäder*†, Siegfried Nitschke‡, Reinhard Stösser‡ and Hans-Hubert Borchert†

†Department of Pharmacy and ‡Department of Chemistry, Humboldt University, Goethestr. 54, 13086, Berlin, Germany

and Abraham Domb

School of Pharmacy, The Hebrew University Jerusalem, Israel

(Revised 28 November 1996)

Spectral spatial electron paramagnetic resonance imaging (e.p.r.i.) was applied to characterize the microenvironment inside 2 mm thick poly(1,3-bis-*p*-carboxyphenoxypropane-*co*-sebacic anhydride) (1/4) polymer discs. Incorporated nitroxides are highly immobilized in the dry polymer. Exposure to 0.1 M phosphate buffer (pH 7.4) resulted in the formation of a front of degraded polymer from outside to inside. The localized measurement of pH values inside the polymer matrix was performed, using a pH sensitive nitroxide (pK_a 6.1). A pH gradient was found between the degrading polymer and the buffer, but also inside the polymer. The pH inside the delivery matrix rises with time for 4.7 to 7.4. The results demonstrate that difficulties in the characterization of the pH, one of the most important parameters for drug delivery and polymer degradation, can be overcome by spectral spatial e.p.r.i. © 1997 Elsevier Science Ltd.

(Keywords: biodegradable polymers; e.p.r. imaging; pH measurement)

INTRODUCTION

Biodegradable polymers are intensively studied as drug delivery systems[1,2]. However, there is still a rather sparse comprehension of the elementary processes involved in the degradation and erosion of these implants, although biodegradable drug delivery systems based on polyesters (e.g. Decapeptyl™ Depot, Enantone™ or Zoladex™) and polyanhydrides (e.g. Gliadel™ or Septecin™) are now in clinical use. The characterization of the microenvironment inside the polymer is an important problem with direct impact on the release kinetics, polymer degradation and finally on therapeutic efficiency. An acidic microenvironment may result from polymer degradation, because polyanhydrides degrade into dicarboxylic acids and polyesters into α-hydroxy acids. However, the prediction of the pH inside the delivery system is difficult due to the influence of several factors such as: the kinetics of water penetration and polymer degradation, acidic/basic properties of the incorporated drugs, the solubilities of incorporated drugs and polymer degradation products, and the diffusion kinetics of the monomers into the release medium and of buffering substances from the release medium into the polymer. Also, these factors are known to be pH dependent, which make predictions even more difficult. For example, polyester degradation is acid catalysed[3], while the degradation of polyanhydrides is decreased in an acidic environment[4].

Although the importance of the pH for drug delivery, polymer degradation and polymer erosion is well accepted, few experimental results have been published due to the difficulties in the assessment of this parameter. Göpferich and Langer[5] demonstrated by confocal microscopy that the pH of the release medium decreases in the vicinity of poly(1,3-bis-*p*-carboxyphenoxypropane-*co*-sebacic anhydride) [P(CPP-SA)] polyanhydride discs by one pH unit[5]. It was concluded that the pH will become even more acidic inside the polymer matrix, although the authors were not able to characterize the microenvironment inside the tablet by their approach. However, the conclusion is experimentally supported by a study of Laurencin *et al.*[6], who inserted a pH sensitive glass electrode into the same polymer, where a pH of 5 was found after exposure to phosphate buffer pH 7.7. High pH gradients between the degraded core of biodegradable polyester cylinders (pH 2) and the buffer (pH 7.4) were described by Herrlinger[7], who used pH sensitive glass microelectrodes.

Disadvantages of pH assessment by glass electrodes

* To whom correspondence should be addressed

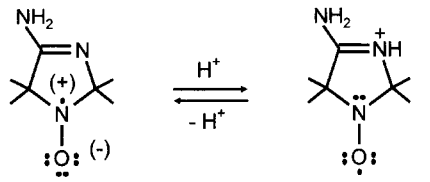

Figure 1 Principle of pH measurement by e.p.r. parameters. Protonation of groups localized near to the nitroxyl moiety induces changes of the spin density at the nitrogen atom of the radical nitroxyl group, which finally leads to different spectroscopic parameters such as the value of hyperfine splitting and the *g* value

include the destructiveness and the lack of spatial information. These drawbacks do not exist for spectroscopic methods based on magnetic resonance, such as nuclear magnetic resonance (n.m.r.) and electron paramagnetic resonance (e.p.r.). Taking advantage of the pH sensitivity of the chemical shift, ^{31}P n.m.r. spectroscopy has been used by Burke[8] to assess the pH of protein loaded poly(lactic-co-glycolic acid) (PLGA) microspheres exposed to sheep serum.

E.p.r. spectroscopy can provide unique information in several fields in pharmacy[9]. Stable nitroxide radicals have now been used for decades as molecular probes for the measurement of microviscosity and micropolarity. A new application was made possible by the synthesis of pH sensitive nitroxides[10]. The principle of pH measurement by e.p.r. is illustrated in *Figure 1*. The protonation of groups localized near the nitroxyl moiety induces

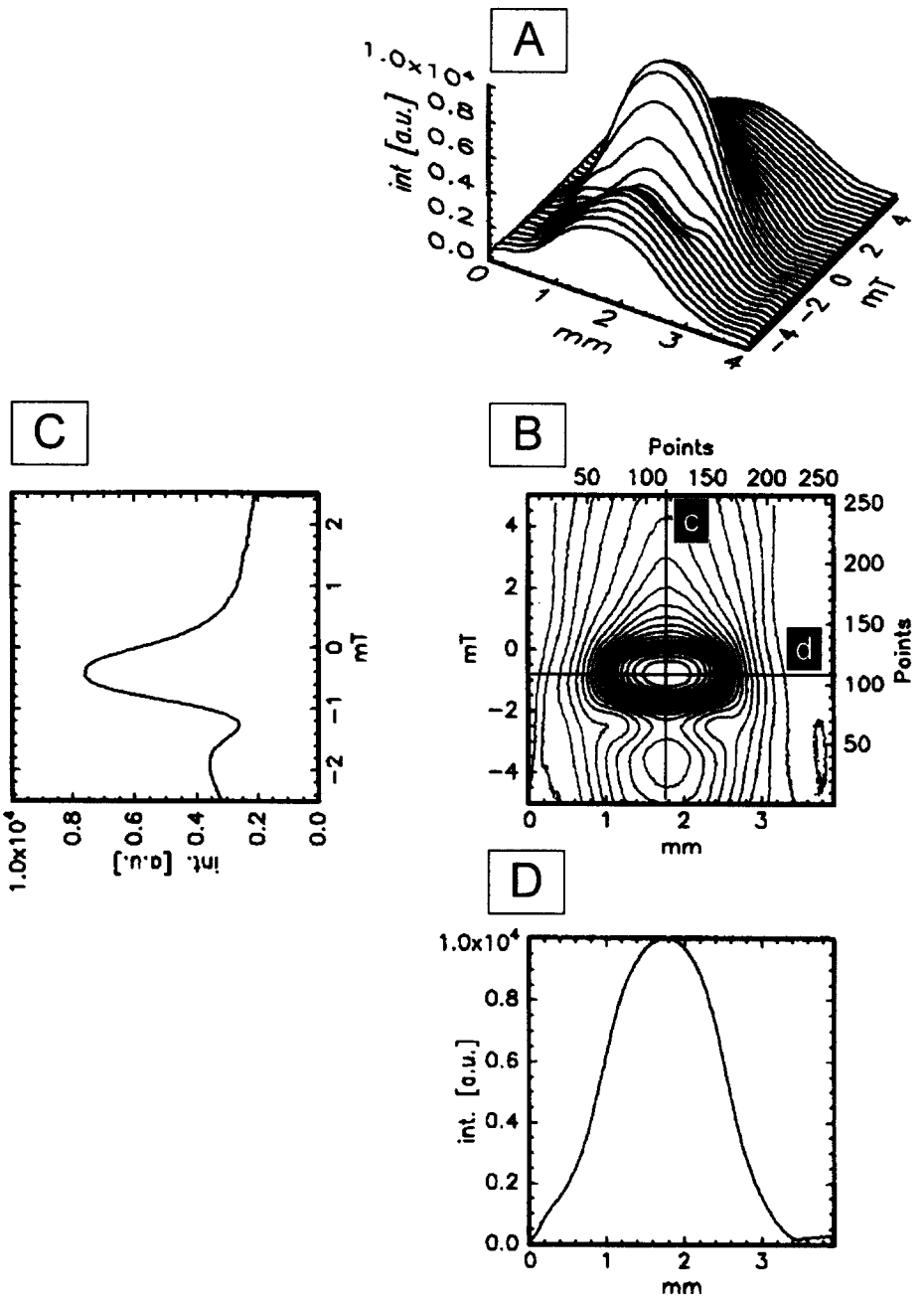

Figure 2 E.p.r. spectral spatial image of a 3-carboxy-2,2,5,5-tetramethyl-pyrrolidine-1-oxyl loaded poly(fatty acid dimer-sebacic acid anhydride) (P(FAD-SA)) polymer 2 mm thick sample (3 mmol kg^{-1} polymer): (A) 3D display; (B) 2D contour plot; (C) e.p.r. spectrum taken from slice c of the image; (D) spatial dimension from slice d of the image

changes of the spin density on the nitrogen atom of the radical nitroxyl group, which finally leads to different spectroscopic parameters such as the value of hyperfine splitting and the g value. The advantageous use of this non-invasive technique has been demonstrated by *in situ* measurement of drug decomposition induced pH changes of the aqueous phase in non-transparent water-in-oil ointments *in vitro*[11]. The development of low frequency spectrometers now permits one to conduct e.p.r. studies on living animals. The first *in vivo* measurement of the pH inside a biodegradable drug delivery system described a polymer degradation induced pH drop from 4 to 2 inside subcutaneously implanted PLGA tablets[12]. E.p.r. has also been used to follow the pharmacological effects of antacids on the stomach pH in living mice[13].

A deeper insight into the mechanism of drug delivery from a polymeric delivery system can be obtained if the information from the e.p.r. spectrum (nitroxide concentration, microviscosity, pH) can be attributed to a particular layer of the delivery system. This can be realized by a special technique called spectral spatial e.p.r. imaging (e.p.r.i.)[14,15], which introduces a spatial dimension by means of additional magnetic gradients. As illustrated in *Figure 2*, images displaying spectral properties as a function of their distribution along one spatial axis are achieved. Information needed for the image is acquired by recording a number of spectra with different values of magnetic field gradients in the field direction. The spatial resolution is limited by technical conditions between the positive and negative gradient maxima.

Although otherwise claimed[16], the first application of spectral spatial e.p.r.i. to follow diffusion processes in polymers dates back to 1991, where the heterogeneity of microviscosity inside biodegradable polyester foils induced by the penetration of water has been demonstrated[17]. It was the aim of the present study to investigate the possibility of localized and non-invasive pH measurement inside biodegradable polymers by spectral spatial e.p.r.i. Due to the clinical importance we decided to investigate the polyanhydride P(CPP-SA) (1/4). This polymer is the biodegradable matrix used in the Gliadel™ brain tumour implant, which is now in clinical use[18]. We selected the spin probe 4-amino-2,2,5,5-tetramethyl-3-imidazoline-1-yloxy (AT, pK_a 6.1), because the pH inside this polymer can be expected to be between 4 and 6.

EXPERIMENTAL

Materials and sample preparation

The spin probe AT was purchased from Professor I. A. Grigoriev (Institute of Organic Chemistry, Russian Academy of Sciences, Novosibirsk, Russia). The polyanhydride P(CPP-SA) (1/4) (M_w 45 000) was synthesized as previously described[19]. The nitroxide loaded discs were manufactured by melt moulding at 100°C into a home-made quartz ring holder with a diameter of 5 mm and 2 mm thickness.

For calibration measurements, the spin probes were solved in a citric acid–phosphate buffer according to McIlvaine (pH adjustment by the use of different ratios of 0.2 M Na_2HPO_4 and 0.1 M citric acid solutions). A quartz flat cell was used for measurement.

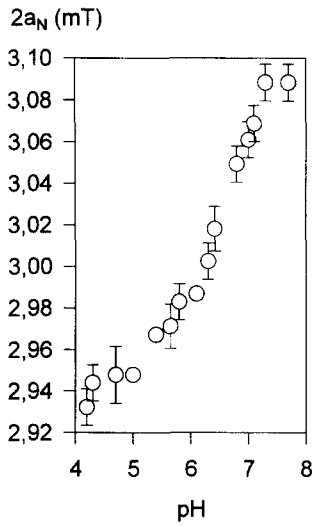

Figure 3 pH calibration curve of AT obtained by spectral spatial e.p.r.

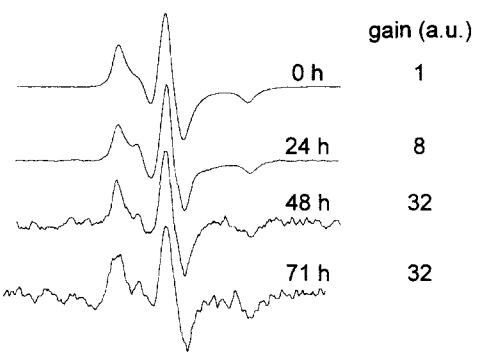

Figure 4 E.p.r. spectra (first derivative) of AT loaded P(CPP-SA) discs exposed to nitroxide free 0.1 M phosphate buffer (pH 7.4)

The discs were placed in 10 ml of nitroxide free or nitroxide containing (1.5 mmol l^{-1}) 0.1 M phosphate buffer (pH 7.4) at 37°C. The buffer was changed daily to assure sink conditions. For measurement, the polymer samples were taken out from the buffer and inserted into the e.p.r. cavity.

E.p.r.i.

The instrumentation used consists of a 9.4 GHz e.p.r. spectrometer which allows one to attach an additional set of two water-cooled combined gradient- and linear-field scan coils in its magnetic air gap, a high current analogue bipolar amplifier for each coil and a personal computer, equipped with boards for driving the amplifiers (D/A converter) and for data acquisition (A/D converter). The field detection Hall probe should be mounted outside the pole gap to prevent magnetic gradients disturbing the field regulation. The image corresponds to a model object, whose coordinates are length, field and signal amplitude. Projections at the first two coordinates are the spatial distribution of the detected species and the gradient free e.p.r. spectrum of the whole sample. The theory assumes the gradient-influenced spectra to be the projections of the object under equidistant angles between $-180°$ and $+180°$. Thus, projection reconstruction algorithms can be applied to obtain the image from data for the measured

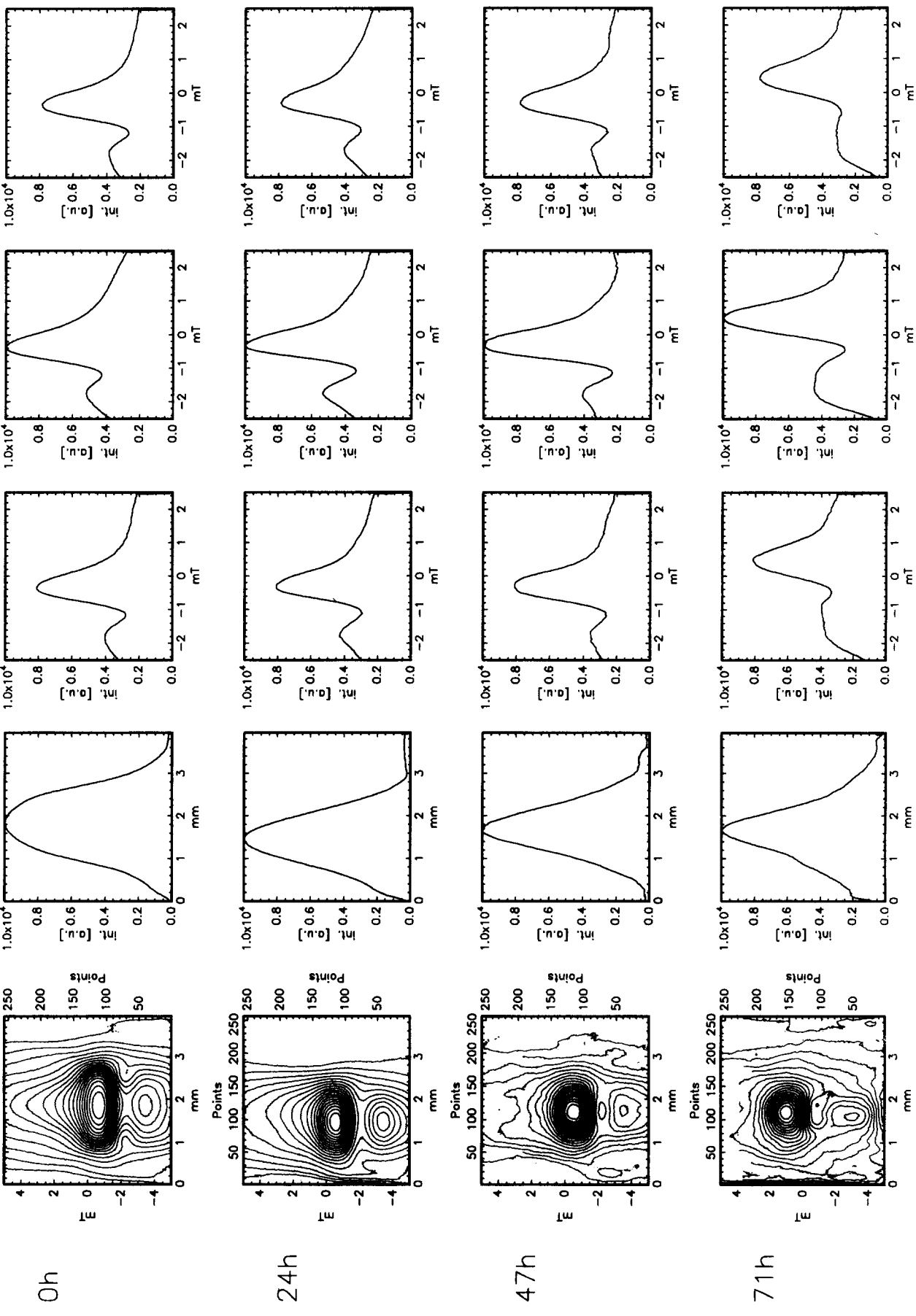

Figure 5 Spectral spatial e.p.r. images of AT loaded P(CPP-SA) discs exposed to nitroxide free 0.1 M phosphate buffer (pH 7.4): (A) 2D spectral spatial contour plot; (B) spatial dimension; (C) e.p.r. spectrum typical for the left outer layers of the polymer disc; (D) e.p.r. spectrum typical for the central layers of the polymer disc; (E) e.p.r. spectrum typical for the right outer layers of the polymer discs

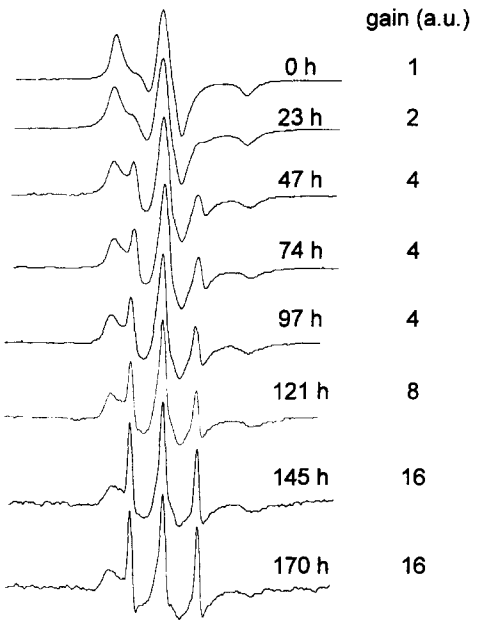

Figure 6 E.p.r. spectra of AT loaded P(CPP-SA) discs exposed to AT containing (1.5 mmol l^{-1}) 0.1 M phosphate buffer (pH 7.4)

spectra. Due to the limited range of realizable gradients the range of angles is also limited. Taking a given number of projections for the whole range, a certain number of them at each end of the range are called 'missing projections'. The algorithm takes that in account.

The e.p.r. spectra were recorded at 9.375 GHz (*X*-band) using an Electron Resonance Spectrometer ERS 220 (Centre of Scientific Instruments, Berlin, Germany) equipped with a rectangular resonator.

The imaging unit developed by us consisted of the following parts:

1. A personal computer with plug-in boards PC 30 and PC 66 (Meilhaus, Pucheim, Germany) for data acquisition and analogue output.
2. Two high current d.c. amplifiers FM 1191 (20 V, 50 A d.c., 3 kHz) (FM-Elektronik, Berlin, Germany).
3. Two water-cooled gradient coils, type ZZG (4 T m^{-1}) (Centre of Scientific Instruments, Berlin, Germany).

The following parameters have been used: sample points per projection, 512; sample time per projection, 5 s; time constant, 0.05 s; maximum gradient, 2.28 T m^{-1}; spatial range, 4 mm; spectral range, 15 mT; central field, 334 mT; microwave power, 1 mW; modulation amplitude, 0.15 mT. Back projection: total number of projections, 95; missing projections, 12; output matrix, 256 × 256.

RESULTS AND DISCUSSION

The calibration curve demonstrates the expected pH sensitivity of the hyperfine splitting (*Figure 3*). The pK_a value of 6.1 agrees well with results obtained by routine e.p.r. spectroscopy[10,12]. The e.p.r. spectra of dry AT loaded P(CPP-SA) discs indicate a high degree of immobilization of the incorporated spin probe (*Figure 4*, 0 h). Exposure of AT loaded P(CPP-SA) discs to nitroxide free buffer (set-up I) leads to a decrease in the signal intensity. However, no changes of the spectral shape were observed. This observation indicates that the amount of water solubilized AT in the P(CPP-SA) is too low to be detected (less than 1% of the total nitroxide concentration as estimated by spectral simulation). Therefore, it can be concluded that incorporated hydrophilic drugs of low molecular weight, once they become water solubilized, diffuse into the buffer very rapidly.

In order to obtain a spatial resolution of the delivery process, spectral spatial e.p.r.i. was performed. There was no difference in the spectral shape of the e.p.r. spectra of AT localized near to the left surface (*Figure 5C*, 0 h), in the central layer (*Figure 5D*, 0 h) and near the right surface (*Figure 5E*, 0 h). Exposure of AT loaded P(CPP-SA) discs to nitroxide free buffer (set-up I) leads to decrease in the spatial dimension with time (*Figure 5*—column B). No pH information can be extracted from the recorded spectra, because no spectral contribution of water solubilized AT molecules was recorded (although the spectral parameters of the non-solubilized AT molecules do also depend to some extent on the acidity of the environment).

In order to measure the pH it was necessary to increase the concentration of water solubilized AT molecules inside the pores of the degrading polymer matrix. This was performed by exposing the AT loaded P(CPP-SA) discs to AT containing (1.5 mmol l^{-1}) phosphate buffer, pH 7.4 (set-up II). This experimental strategy led to a decreased or diminished AT concentration gradient between the eroding polymer and the buffer, while the concentration gradients remained unchanged for the monomers SA and CPP. The e.p.r. spectra show remarkable differences to those recorded with the first set-up (*Figure 6*). A spectral contribution of rapidly tumbling nitroxide molecules becomes visible with time, characterized by a spectrum of three narrow lines. The contribution of the mobile part to the e.p.r. spectrum increases with time and becomes predominant after five days. However, due to the narrower linewidth of rapidly tumbling nitroxides, the signal amplitude will be approximately 5–10 times higher for a given nitroxide concentration compared to that of immobilized molecules. Preliminary results for spectral simulation studies suggest that the concentrations of immobilized and mobile nitroxide molecules are comparable until the end of the study. The results of e.p.r. spectroscopy prove the formation of low viscous compartments with time. However, they give no hints whether these compartments are formed homogeneously or inhomogeneously in the polymer.

This question was successfully answered by spectral spatial e.p.r.i. A front penetrating from outside to inside can be seen on the images (*Figure 7*). Differences in the spectral shape between the outer layers and the core start to develop after one day and become clearly visible after two days. While the e.p.r. spectra of the core remained unchanged during the first days, the spectral shape of the outer layers derived from a superposition of nitroxide molecules with a different motional state, namely immobilized and highly mobile. It has been shown by microscopic techniques *in vitro*[20] and by MRI *in vitro* and *in vivo*[21] that P(CPP-SA) erosion is not pure surface erosion, because a porous layer of degraded polymer remains around an intact core. This mechanism has been defined as a surface erosion front mechanism by Mathiowitz *et al.*[20]. It has also been observed by X-ray

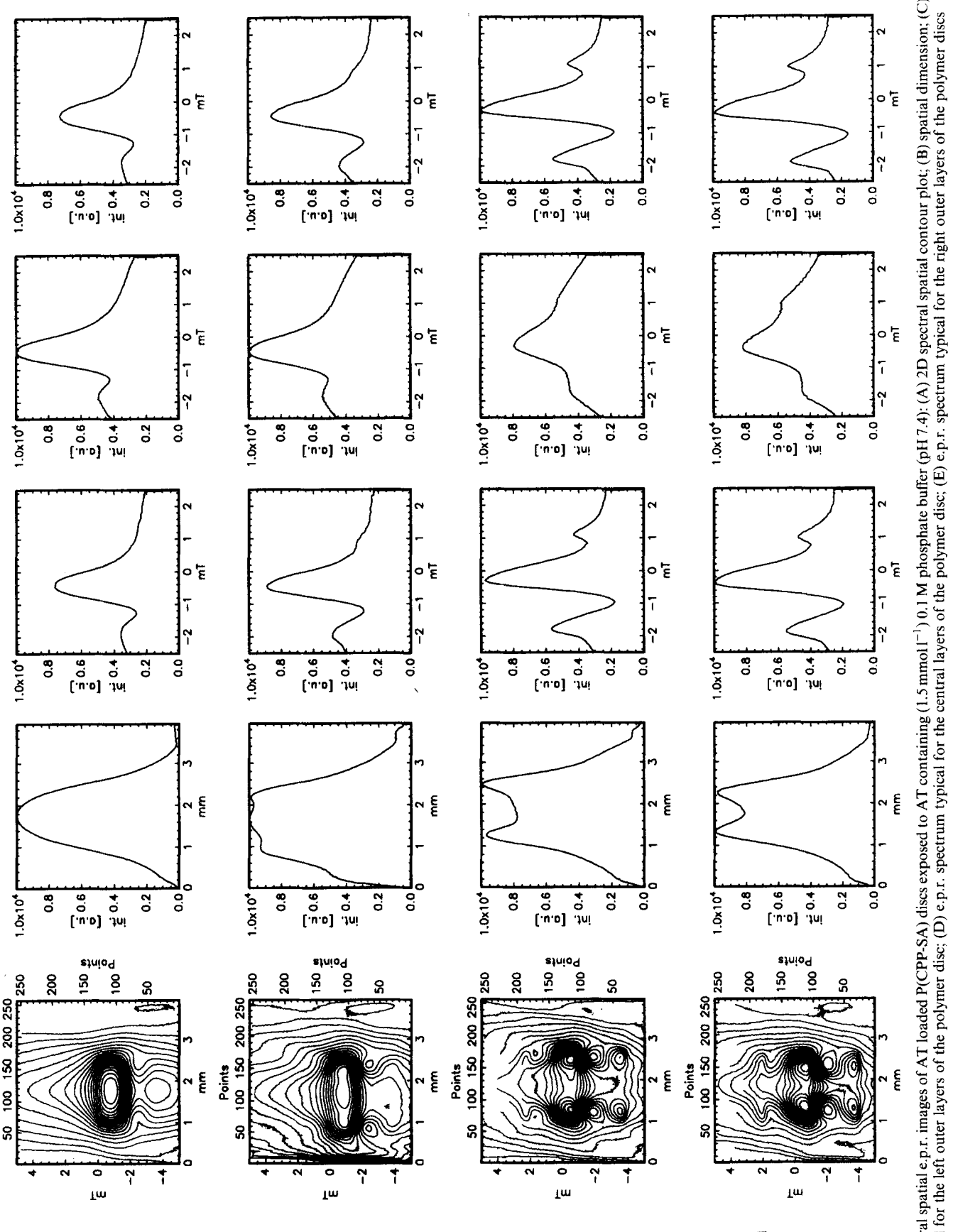

Figure 7 Spectral spatial e.p.r. images of AT loaded P(CPP-SA) discs exposed to AT containing (1.5 mmol l^{-1}) 0.1 M phosphate buffer (pH 7.4): (A) 2D spectral spatial contour plot; (B) spatial dimension; (C) e.p.r. spectrum typical for the left outer layers of the polymer disc; (D) e.p.r. spectrum typical for the central layers of the polymer disc; (E) e.p.r. spectrum typical for the right outer layers of the polymer discs

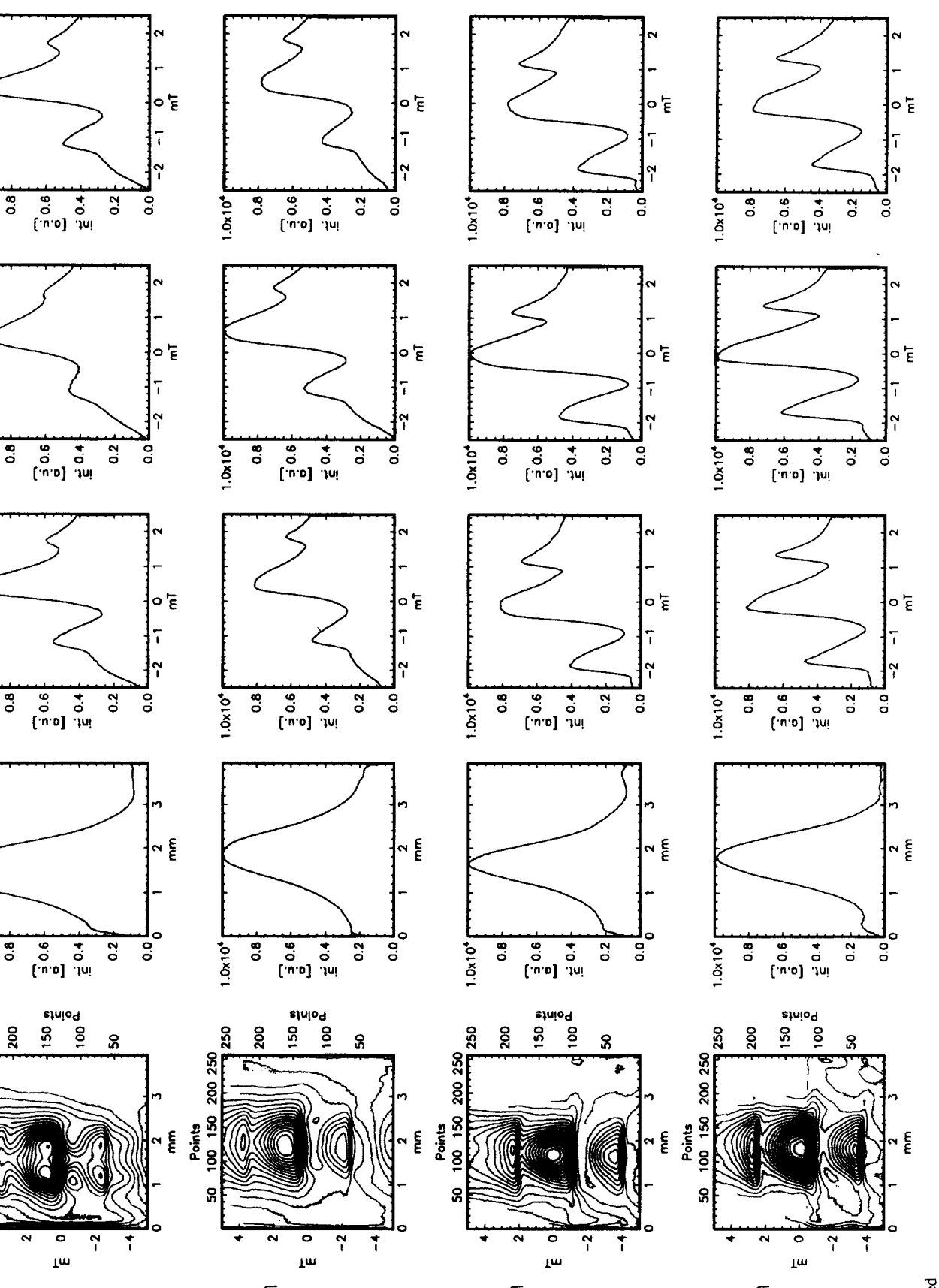

Figure 7 Continued

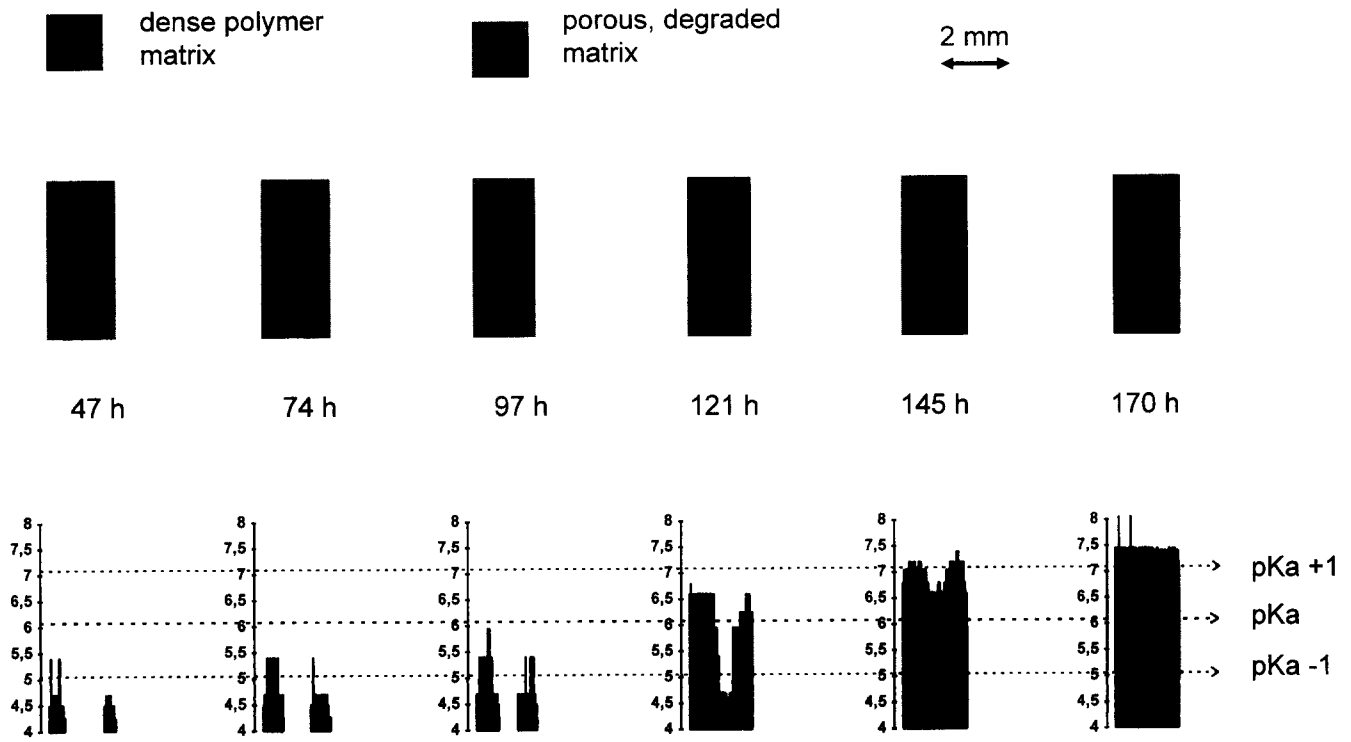

Figure 8 Scheme of polymer degradation (top) and pH values inside degrading P(CPP-SA) (bottom) polymers

diffraction that monomer crystallization occurs inside degrading P(CPP-SA) polymers due to the low water solubility of the monomers SA and CPP[5]. It is, therefore, concluded that the highly mobile nitroxide molecules are solubilized in the water filled pores, while the immobilized nitroxides are localized in the degraded polymer layer or are coprecipitated with the monomers SA and CPP. From the distance between the first and the third peak ($2a_N$), the pH value of a particular layer can be measured. The time evolution of the degradation process and pH values inside the polymer matrix are illustrated in *Figure 8*. The first reliable measurement of pH values of the outer layers is possible after two days. The experimental data indicate an acidic environment with a pH of 4.7. The polymer degradation front proceeds with time and reaches the centre after five days. Furthermore, an increase in the pH inside the polymer can be observed with time, starting from outside to inside. A pH gradient of more than 1.5 units between the outer layers (pH 6.5) and the disc centre (pH 4.7) was found after five days. A smaller pH gradient was detectable at day 6. At day 7, the pH gradient was no longer observable and the pH inside the polymer pores reached 7.4, the value of the phosphate buffer.

In order to understand the factors which determine the microenvironment inside a biodegradable polymer it is important to know if substances from the surrounding environment are able to diffuse into the polymer and how fast this may occur. Therefore, a third experimental set-up was developed to answer the question, and plain P(CPP-SA) polymers were exposed to AT containing buffer solution. The e.p.r.i. data demonstrate that AT is able to penetrate from outside to inside into the polymer with time (*Figure 9*). The penetration front proceeded with zero order kinetics with a velocity of $0.30\,\text{mm}\,\text{day}^{-1}$ ($r^2 = 0.99764$). From the shape of the e.p.r. spectra, a large amount of immobilized nitroxide molecules can be concluded to be present. The data suggest that hydrophilic compounds of low molecular weight penetrating into eroding P(CPP-SA) polymers may become immobilized by coprecipitation.

In summary, it was demonstrated that hydrophilic drugs of low molecular weight were released from outside to inside from P(CPP-SA) polymers, confirming a close relation between polymer erosion and drug release. We confirmed the zero order kinetics of polymer erosion and proved for the first time the possibility of the localized assessment of pH values inside degrading drug delivery systems by spectral spatial e.p.r.i. An acidic pH of 4.7 was observed in the early stage of degradation. With time, the pH increased and finally reached the pH of the buffer solution. We attribute the observed pH increase to the diffusion of the acidic monomers SA and CPP into the buffer and the diffusion of phosphate ions from the buffer into the degrading polymer matrix. Furthermore, we are providing the first direct experimental evidence of pH gradients inside biodegradable polymers. We propose that experimental difficulties in the characterization of one of the most important parameters for drug stability, drug delivery kinetics and polymer degradation can be overcome by the use of the non-invasive method of spectral spatial e.p.r.i.

ACKNOWLEDGEMENTS

The authors thank Dr Uwe Ewert for his advice and for the permission to use his software. K. M. gratefully acknowledges his support from Deutsche Forschungsgemeinschaft (DFG grant MA1648). This work was supported in part by NCDDG grant No. CA52857.

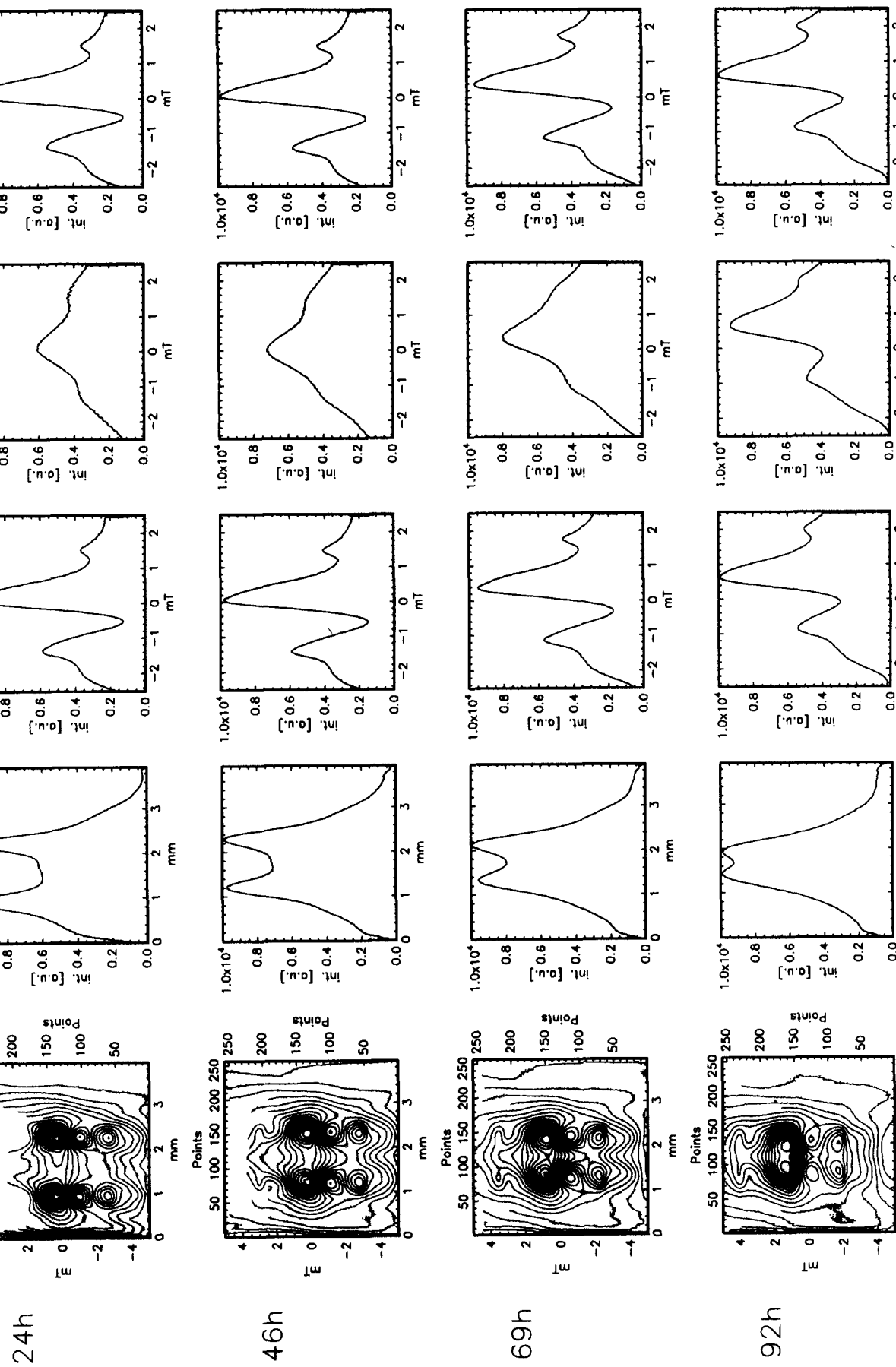

Figure 9 Spectral spatial e.p.r. images of plain P(CPP-SA) discs exposed to AT containing (1.5 mmol l^{-1}) 0.1 M phosphate buffer (pH 7.4): (A) 2D spectral spatial contour plot; (B) spatial dimension; (C) e.p.r. spectrum typical for the left outer layers of the polymer disc; (D) e.p.r. spectrum typical for the central layers of the polymer discs; (E) e.p.r. spectrum typical for the right outer layers of the polymer disc

REFERENCES

1. Domb, A. J., Amselem, S. and Maniar, M., in *Polymeric Biomaterials*, ed. S. Dumitriu. Marcel Dekker, New York, 1994, p. 399.
2. Domb, A. J. (ed.), *Polymeric Site-specific Pharmacotherapy*. Wiley, Chichester, UK, 1994.
3. Göpferich, A., in *Handbook of Biodegradable Polymers*, ed. A. Domb, J. Kost and D. Wiseman, 1996, **36,** 694.
4. Leong, K. W., Brott, B. C. and Langer R., *J. Biomed. Mat. Res.*, 1985, **19,** 941.
5. Göpferich, A. and Langer, R., *J. Polym. Sci., Part A: Polym. Chem.* 1993, **31,** 2445.
6. Laurencin, C. T., Domb, A. J., Morris, C. and Langer, R., *Proc. Intern. Symp. Contr. Rel. Bioact. Mat.*, 1988, **15,** 248.
7. Herrlinger, M., *In vitro* Polymerabbau und Wirkstofffreigabe von Poly-DL-Laktid-Formlingen. Thesis, Heidelberg, 1994, p. 125.
8. Burke, P. A., *Proc. Soc. Contr. Rel.*, 1996, **23,** 133.
9. Mäder, K., Swartz, H. M., Stösser, R. and Borchert, H.-H., *Pharmazie*, 1994, **49,** 97.
10. Khramtsov, V. V. and Weiner, L. M., in *Imidazoline Nitroxides*, Vol. 2, ed. L. B. Volodarsky. CRC Press, Boca Raton, FL, 1988, p. 37.
11. Kroll, C., Mäder, K., Stoesser, R. and Borchert, H.-H., *Europ. J. Pharm. Sci.*, 1995, **3,** 21.
12. Mäder, K., Gallez, B., Liu, K. J. and Swartz, H. M., *Biomaterials*, 1986, **17,** 459.
13. Gallez, B., Mäder, K. and Swartz, H. M., *Magn. Res. Med.*, 1997, **86,** 126.
14. Ewert, U. and Herrling, T., *Chem Phys. Lett.*, 1986, **129,** 516.
15. Eaton, G. R. and Eaton, S. S., *Concepts Magn. Res.*, 1995, **7,** 149.
16. Schlick, S., Pilar, J., Kweon, S. C., Vacik, J., Gao, Z. and Labsky, J., *Macromolecules*, 1995, **28,** 5780.
17. Mäder, K., Borchert, H.-H., Stößer, R., Groth, N. and Herrling, T., *Pharmazie*, 1991, **46,** 439.
18. Brem, H., Piantadosi, S., Burger, P. C., Walker, M., Selker, R., Vick, N. A., Black, K., Sisti, M., Brem, S., Mohr, G., Müller, P., Morawetz, R. and Schold, S. C., *Lancet*, 1995, **345,** 1008.
19. Domb, A. J. and Langer, R., *J. Polym. Sci.*, 1987, **25,** 3373.
20. Mathiowitz, E., Jacob, J., Pekarek, K. and Chickering, D. III, *Macromolecules*, 1993, **26,** 6756.
21. Mäder, K., Bacic, G., Domb, A., Elmalak, O., Langer, R. and Swartz, H. M., *J. Pharm. Sci.*. Gordon and Breach Science Publishers, Amsterdam, 1997 (in press).